

See discussions, stats, and author profiles for this publication at: <https://www.researchgate.net/publication/47741514>

# Cancer Drug-Resistance and a Look at Specific Proteins: Rho GDP-Dissociation Inhibitor 2, Y-Box Binding Protein 1, and HSP70/90 Organizing Protein in Proteomics Clinical Applicatio...

ARTICLE in JOURNAL OF PROTEOME RESEARCH · NOVEMBER 2010

Impact Factor: 4.25 · DOI: 10.1021/pr100468w · Source: PubMed

CITATIONS

11

READS

19

12 AUTHORS, INCLUDING:



[Helena Skalnikova](#)

Academy of Sciences of the Czech Republic

18 PUBLICATIONS 279 CITATIONS

[SEE PROFILE](#)



[Rita Sucha \(Hrabakova\)](#)

Academy of Sciences of the Czech Republic

9 PUBLICATIONS 47 CITATIONS

[SEE PROFILE](#)



[Marta Dziechciarkova](#)

Palacký University of Olomouc

19 PUBLICATIONS 334 CITATIONS

[SEE PROFILE](#)



[Ola Forsstrom-Olsson](#)

Ludesi AB

3 PUBLICATIONS 29 CITATIONS

[SEE PROFILE](#)

# Cancer Drug-Resistance and a Look at Specific Proteins: Rho GDP-Dissociation Inhibitor 2, Y-Box Binding Protein 1, and HSP70/90 Organizing Protein in Proteomics Clinical Application

Helena Skalnikova,<sup>†,‡</sup> Jirina Martinkova,<sup>†,‡</sup> Rita Hrabakova,<sup>†</sup> Petr Halada,<sup>‡</sup>  
Marta Dziechciarkova,<sup>§</sup> Marian Hajduch,<sup>§</sup> Suresh Jivan Gadher,<sup>||</sup> Andreas Hammar,<sup>⊥</sup>  
Daniel Enetoft,<sup>⊥</sup> Andreas Ekefjard,<sup>⊥</sup> Ola Forsstrom-Olsson,<sup>⊥</sup> and Hana Kovarova<sup>\*,†</sup>

*Institute of Animal Physiology and Genetics AS CR, v.v.i., Rumburska 89, 277 21 Libechov, Czech Republic,  
Institute of Microbiology AS CR, v.v.i., Videnska 1083, 142 20 Prague, Czech Republic, Laboratory of  
Experimental Medicine, Institute of Translational and Molecular Medicine, Faculty of Medicine and Dentistry,  
Palacky University and University Hospital, Puskinova 6, 775 20 Olomouc, Czech Republic,  
Millipore Bioscience, 15 Research Park Drive, St. Charles, Missouri 63304, United States, and Ludesi,  
Engelbrektsgratan 15, SE-211 33 Malmö, Sweden*

Received May 14, 2010

Resistance to anti-cancer drugs is a well recognized problem and very often it is responsible for failure of the cancer treatment. In this study, the proteome alterations associated with the development of acquired resistance to cyclin-dependent kinases inhibitor bohemine, a promising anti-cancer drug, were analyzed with the primary aim of identifying potential targets of resistance within the cell that could pave a way to selective elimination of specific resistant cell types. A model of parental susceptible CEM T-lymphoblastic leukemia cells and its resistant counterpart CEM-BOH was used and advanced 2-D liquid chromatography was applied to fractionate cellular proteins. Differentially expressed identified proteins were further verified using immunoblotting and immunohistochemistry. Our study has revealed that Rho GDP-dissociation inhibitor 2, Y-box binding protein 1, and the HSP70/90 organizing protein have a critical role to play in resistance to cyclin-dependent kinases inhibitor. The results indicated not only that quantitative protein changes play an important role in drug-resistance, but also that there are various other parameters such as truncation, post-translational modification(s), and subcellular localization of selected proteins. Furthermore, these proteins were validated for their roles in drug resistance using different cell lines resistant to diverse representatives of anti-cancer drugs such as vincristine and daunorubicin.

**Keywords:** cancer • anti-cancer drugs • drug resistance • CEM T-lymphoblastic leukemia • CDK inhibitor • proteomics • Rho GDP-dissociation inhibitor 2 • Y-box binding protein 1 • Hsp70/90 organizing protein • biomarker

## Introduction

Cancers represent group of unprecedentedly heterogeneous diseases that affect humans with high frequency and contribute significantly to overall morbidity and mortality. Development of resistance to cancer chemotherapeutic treatments is a major problem for successful therapy, especially in late stages of the disease.

Cancer cells can acquire drug resistance by several distinct mechanisms. One such group of mechanisms of extreme importance is represented by pharmacological and physiologi-

cal parameters. Included within this group is the family of P450 enzymes in liver which controls the metabolism of drugs. Increased levels of these enzymes are observed in a variety of solid tumors and may contribute to drug resistance. The membrane proteins including channels, solute carriers, and ABC transporters are known to play a role in increased drug efflux from cancer cells. Inadequate metabolic activation of anti-cancer drug analogues of DNA precursors represents a synergistic enhancement to the drug resistance by cancer cells. Furthermore, the resistance to the drugs that directly affect structural integrity of DNA may result from the activation of DNA-repair systems which may nullify the effect of the drug. The second mechanism grouping of the factors contributing to the anti-cancer drug resistance includes altered survival pathways such as evasion of apoptosis, necrosis, mitotic catastrophe, or senescence.<sup>1,2</sup> Consideration has to be given to a third group represented by cancer stem cells. These cells are likely to share many of the properties of normal stem cells,

\* To whom correspondence should be addressed. E-mail, kovarova@iapg.cas.cz; tel, +420 315 639 582; fax, +420 315 639 510.

<sup>†</sup> Both authors contributed equally to this work.

<sup>‡</sup> Institute of Animal Physiology and Genetics AS CR, v.v.i.

<sup>§</sup> Institute of Microbiology AS CR, v.v.i.

<sup>||</sup> Palacky University and University Hospital.

<sup>⊥</sup> Millipore Bioscience.

<sup>⊥</sup> Ludesi.

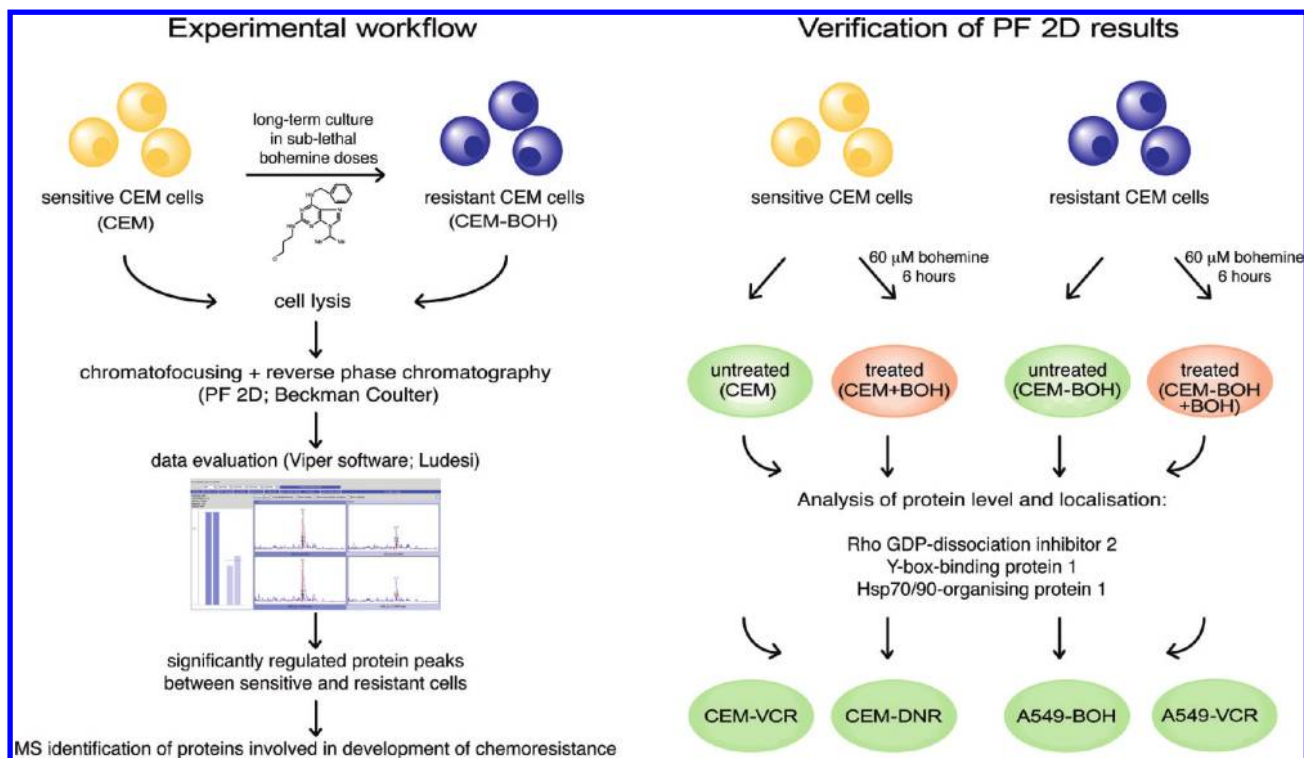


**Figure 1.** Schematic presentation of the experimental and verification workflows. The lysates of cell samples of parental susceptible CEM cell line and CEM-BOH cells resistant to cyclin-dependent kinases inhibitor bohemia were fractionated using 2-D liquid chromatography. The proteome maps were evaluated for differentially expressed protein peaks and identity of the proteins was determined by mass spectrometry. Selected protein changes were verified using immunoblotting and immunohistochemistry. The proteins were further validated for their roles in drug resistance using CEM and A549 cell lines resistant to vincristine or daunorubicin.

thus, mediating self-renewal and long life span including resistance to drugs and toxins through the expression of several ABC transporters, an active DNA-repair capacity, and a resistance to apoptosis.<sup>3</sup> Most of the above-described mechanisms were revealed using cell culture experiments and their correlation to clinical outcomes need further studies.

Recently, proteomic approaches have been applied to further our knowledge of the mechanisms underlying chemoresistance in context of overall protein expression and disease states. Such studies have been performed to date on selected cancer cell lines to address resistance to drugs including DNA damaging agents (doxorubicin, cisplatin, carboplatin, etoposide, daunorubicin, mitoxantrone) and drugs targeting microtubule dynamics (vincristine, vinblastine). Although the conventional 2-DE was utilized in most of these studies resulting predominantly in identification of abundant proteins, many particular mechanisms of resistance were identified for individually selected drugs and cancer cell lines with a commonality of several other features. Among them, the up-regulated expressions of HSP27, 14-3-3 $\sigma$ , and peroxiredoxins were evident and were further validated (reviewed in Zhang and Liu).<sup>2</sup> However, most of the proteins identified in the proteomic analyses of drug resistant cancer cells have not been verified for their expression changes using other approaches such as Western blot or for their prominent role in drug resistance using functional assays such as MTT cytotoxicity and colony formation.

Previously, we described the effects of bohemia, an inhibitor of cyclin-dependent kinases (CDKI) from the family of trisubstituted purines, on primarily sensitive T-lymphoblastic leukemia CEM cells as well as resistant lung adenoma cell line A549.<sup>4,5</sup> The cyclin-dependent kinases together with cyclins

belong to the key molecules regulating cell cycle progression and numerous compounds that can suppress cyclin/cyclin-dependent kinases activities have been described as cytostatic drugs.<sup>6</sup> On the basis of the evaluation of the protein maps and possible pathways relevant to response to CDKI, the glycolytic enzymes, annexin IV, histones, and the Crkl adaptor protein implicated in many signal transduction events appeared to be the important targets. The level and phosphorylation of Crkl protein, which is the major tyrosine-phosphorylated protein in chronic myeloid leukemia, was down-regulated in CDKI treated CEM T-lymphoblastic leukemia cells. These changes were validated using immunoblot experiments and in our pilot experiments using K562 myeloid leukemia cells transplanted into SCID mice and treated/untreated with CDKI under *in vivo* conditions.<sup>4</sup>

In this study, the proteome alterations associated with the development of acquired resistance to CDKI bohemia were analyzed on a model of parental susceptible CEM cell line and its resistant counterpart CEM-BOH. 2-D liquid chromatography was used for protein fractionation of cell lysates. The proteome maps were evaluated for differentially expressed proteins and selected changes were further verified using immunoblotting and immunohistochemistry. Furthermore, the proteins were validated for their roles in drug resistance using different cell lines resistant to diverse representatives of anti-cancer drugs such as vincristine and daunorubicin (Figure 1).

## Materials and Methods

**Chemicals.** Urea, Tris-base, thiourea, sodium dodecyl sulfate (SDS), *n*-octyl glucoside, Tris (2-carboxyethyl) phosphine hydrochloride, and iminodiacetic acid were obtained from Sigma-

Aldrich (St. Louis, MO). Nonidet P40, 3-3(cholamidolpropyl)-dimethylammonio-1-propane sulfonate and dithiothreitol were from USB Corporation (Cleveland, OH). Glycerol and  $\beta$ -glycerolphosphate were purchased from Penta (Prague, Czech Republic). Protease inhibitors cocktail was obtained from Roche (Mannheim, Germany). All other chemicals for protein fractionations were of HPLC or analytical grade and buffers were prepared using Mili-Q water system (Millipore Bedford, MA). Unless otherwise specified, all chemicals used for mass spectrometry were from Sigma (Steinheim, Germany).

**Cell Cultures and Sample Preparation.** The CEM (CEM-CCRF, human T-lymphoblastic leukemia cells) and A549 (human lung adenocarcinoma) cell lines were obtained from American Tissue Culture Collection (ATCC, Manassas, VA). The CEM and A549 cells were cultured in RPMI 1640 and DMEM, respectively, with 5 g/L glucose, 2 mM glutamine, 100 U/mL penicillin, 100  $\mu$ g/mL streptomycin, and 10% fetal calf serum as described previously.<sup>5</sup> The CEM-BOH bulk cell line resistant to CDKI bohemine was derived from parental sensitive CEM cells by selective pressure of CDKI bohemine as described in previous study.<sup>7</sup> The process of selection started with the drug concentration equal to 10% tumor cells survival of parental CEM line and the concentration of the drug was subsequently increased to 10-fold of 50% tumor cells survival. The CEM cells resistant to vincristine (CEM-VCR) or daunorubicin (CEM-DNR) as well as A549 cells resistant to CDKI bohemine (A549-BOH) or vincristine (A549-VCR) were established using the same protocol and drug resistant lines were designated as the bulk culture and grown in the media mentioned above.<sup>7</sup>

For 2-D liquid chromatography fractionation on ProteomeLab PF 2D (PF 2D; Beckman Coulter, Fullerton, CA), parental sensitive CEM cells and resistant counterparts CEM-BOH were grown to approximately  $80 \times 10^6$  cells, harvested, and washed three times with PBS. A total of 400  $\mu$ L of cell suspensions was lysed in 1.6 mL of PF 2D lysis buffer containing 7.5 M urea, 2.5 M thiourea, 62.5 mM Tris, 2.5% octyl glucoside, 6.25 mM TCEP, 12.5% glycerol, and 1.25 mM protease inhibitor. The lysates were centrifuged at 20 000g at 4 °C for 1 h. The supernatants were stored at -80 °C for future use. Two biological replicates of each sample of CEM cells as well as CEM-BOH cells were analyzed. For SDS-PAGE followed by Western blot, parental sensitive CEM cells and their resistant counterparts CEM-BOH, CEM-VCR, and CEM-DNR as well as parental A549 cells and derived resistant cells A549-BOH or A549-VCR were grown in media as mentioned above. The cells were washed in ice-cold PBS, lysed in SDS sample buffer, and boiled and total cell protein extracts of  $10^5$  cells corresponding to approximately 10  $\mu$ g of proteins were loaded on the gel. Additionally, CEM cells treated with 60  $\mu$ M CDKI bohemine for 6 h were prepared in the same manner.

**Two-Dimensional HPLC ProteomeLab PF 2D Chromatography and Image Analysis.** Samples of CEM and CEM-BOH cell lines in denaturing buffer were loaded on PD10 column equilibrated with 25 mL of the start buffer (provided in PF 2D kit, Beckman Coulter, Fullerton, CA) to exchange denaturing lysis buffer to the start buffer. The protein concentration in the sample collected from PD10 column was determined by direct measurement of absorbance at 280 nm (DU 7400 spectrophotometer, Beckman Coulter, Fullerton, CA). For the first-dimension high-performance chromatofocusing fractionation (HPCF), two buffers, a start buffer pH 8.5 and an elution buffer pH 4.0, both provided in PF 2D kit were used to generate an internal linear pH gradient on the column. The HPCF

column was equilibrated with 30 column volumes of start buffer and cell lysate of 3.6 mg of total protein was applied on HPCF column using 5 mL injection loop. The separation was performed at a flow rate of 0.2 mL/min. Once the pH in the column achieved a stable value of 8.5 (30 min), the linear gradient of elution buffer to pH of 4 was switched. The proteins remaining on the column at pH 4 were washed out by 1 M NaCl in 30% *n*-propanol solution. UV detection was performed at 280 nm and the pH of the effluent was monitored using a flow-through online pH probe. Fraction collection started when gradient reached pH 8.3 and individual fractions were collected in 0.3 pH intervals. In every run, pH was monitored for 150 min and UV was monitored for 220 min. In total, 15 fractions collected in the pH range 8.30–4.10 and one fraction collected in the pH > 8.30 (proteins that did not bind to the HPCF column) were collected during HPCF separation. The pH fractions were further separated on high-performance reversed phase column (HPRP) packed with C18 nonporous silica beads. Solvent A was 0.1% trifluoroacetic acid (TFA) in water and solvent B was 0.08% TFA in acetonitrile (MeCN). The separation was done at 50 °C at a flow rate 0.75 mL/min. The gradient was run from 0% to 100% B in 35 min, followed by 100% B for 4 min and 100% A for 10 min. UV absorptions were monitored at 214 nm. The fractions were collected in 0.13 min time intervals into 96-deep well plates using the fraction collector Gilson FC204 (Immunotech a.s., Prague, Czech Republic) and stored at -80 °C until further use.

2-D protein expression maps of sensitive CEM and resistant CEM-BOH cells displaying protein isoelectric point versus protein hydrophobicity were generated by ProteoVue software running on PF 2D system. ProteoVue software converts the UV peak intensity in the chromatograms from the second dimension HPRP column of each pH fraction to a band and line format and provides the mean to view and quantify protein levels. The novel Viper software version 2.3.0.0. was further used to evaluate protein maps. The above software was developed in collaboration with Ludesi (Malmö, Sweden), Beckman Coulter (Fullerton, CA), Johns Hopkins University (Baltimore, MD), and Academy of Sciences of the Czech Republic (Prague, Czech Republic). It is an analysis software for aligning, quantifying, normalizing, and comparing data in a multisample 2-D LC-experiment as described. At first, the baseline in chromatograms was detected and one sample was selected as a Master. Then, the UV profiles of fractions with corresponding pH were aligned to correct eventual pH shifts during the first-dimension separation. The second-dimension chromatograms of each consecutive pH fraction in the Master were then aligned to detect protein peaks eluting in the same retention time. The maximum span of the single protein peak in sequential pH fractions was set to 3 fractions. The second-dimension chromatograms of individual pH fractions of the samples were then aligned with the Master. Protein peaks were detected in the area of retention times from 10 to 26 min and the peak intensities were quantified and normalized to the sum of areas under the chromatograms in this retention time range for the whole sample (in all pH fractions). Additionally, for individual peak areas detected in each of the pH fractions, the Viper software allows calculation of total area for every protein peak with the same retention time that is present in several sequential pH fractions. The peaks with *p*-values in ANOVA test below 0.05 and/or peaks with fold change  $\geq 1.6$  were



**Table 1.** Differentially Expressed Proteins Identified in 2-D LC Experiment<sup>a</sup>

peak no.	protein name	UniProt no.	biological function	change	fold change	p-value
088	Tubulin-specific chaperone A	TBCA_HUMAN	protein folding	↓	2	0.056
115	Rho GDP-dissociation inhibitor 1	GDIR_HUMAN	Rho protein signal transduction	↑	2.02	0.22
	Tumor protein D54	TPD54_HUMAN	regulation of cell proliferation			
	Tropomyosin alpha-3 chain	TPM3_HUMAN	cellular component movement			
	Histone H2B type 1-B	H2B1B_HUMAN	nucleosome assembly			
163	Histone H2A type 1-H*	H2A1H_HUMAN	nucleosome assembly	↓	1.92	0.039
	Elongation factor 1-alpha 1	EF1A1_HUMAN	translational elongation			
200	Stress-induced-phosphoprotein 1	STIP1_HUMAN	response to stress	↑	8.18	0.008
	Macrophage-capping protein	CAPG_HUMAN	protein complex assembly			
362	Rho GDP-dissociation inhibitor 2	GDIR2_HUMAN	actin cytoskeleton organization	↑	2.36	0.591
			Rho protein signal transduction			
365	Tropomyosin alpha-4 chain	TPM4_HUMAN	cellular component movement	↑	1.72	0.046
	Histone H4*	H4_HUMAN	nucleosome assembly			
648	60S ribosomal protein L6*	RL6_HUMAN	translation	↓	2.06	0.18
	60S ribosomal protein L4	RL4_HUMAN	translation			
	Histone H2B type 1-D	H2B1D_HUMAN	nucleosome assembly			
	Histone H4*	H4_HUMAN	nucleosome assembly			
649	Histone H2B type 1-J	H2B1J_HUMAN	nucleosome assembly	↓	2.4	0.006
	Histone H4	H4_HUMAN	nucleosome assembly			
701	Nuclease sensitive element-binding protein 1	YBOX1_HUMAN	regulation of transcription	↓	8.72	0.31
			mRNA processing			
770	60S ribosomal protein L15	RL15_HUMAN	translation	↓	2.56	0.59
	40S ribosomal protein S8	RS8_HUMAN	translation			
780	40S ribosomal protein S24	RS24_HUMAN	translation	↓	1.82	0.107
800	40S ribosomal protein S25	RS25_HUMAN	translation	↑	1.62	0.006
	40S ribosomal protein S4, X isoform	RS4X_HUMAN	translation			
	Small nuclear ribonucleoprotein Sm D3	SMD3_HUMAN	mRNA processing, RNA splicing			
847	Nuclease sensitive element-binding protein 1	YBOX1_HUMAN	regulation of transcription	↓	2.68	0.13
			mRNA processing			
	60S ribosomal protein L26	RL26_HUMAN	translation			
889	Histone H2A type 1-H*	H2A1H_HUMAN	nucleosome assembly	↑	1.67	0.025
1145	60S ribosomal protein L6*	RL6_HUMAN	translation	↓	2.04	0.15
	40S ribosomal protein S13	RS13_HUMAN	translation			
	60S ribosomal protein L7a	RL7A_HUMAN	translation			

<sup>a</sup> The arrows indicate change in the protein level in the resistant cells compared to sensitive cells. Detailed data from MS identification are supplied in the Supplemental Table 1. Asterisks (\*) indicate proteins found in nonsequential fractions.

considered as significant differences and the corresponding fractions were processed by mass spectrometry (Table 1).

**Protein Identification by MALDI-TOF Mass Spectrometry.** The fractions from the second dimension of PF2D separation were completely dried using a SpeedVac and redissolved in 50  $\mu$ L of a cleavage buffer containing 0.01% 2-mercaptoethanol, 50 mM 4-ethylmorpholine acetate, 5% MeCN, and 5 ng of sequencing grade trypsin (Promega, Madison, WI). After overnight digestion, the resulting peptides were acidified by the addition of 5  $\mu$ L of 5% TFA in MeCN. A solution of  $\alpha$ -cyano-4-hydroxycinnamic acid in aqueous 50% MeCN/0.2% TFA (5 mg/mL) was used as a MALDI matrix. A 0.5  $\mu$ L of a sample was deposited on the MALDI target and allowed to air-dry at room temperature. After complete evaporation, 0.5  $\mu$ L of the matrix solution was added. MALDI mass spectra were measured on an Ultraflex III instrument (Bruker Daltonics, Bremen, Germany) equipped with a Smartbeam solid state laser and LIFT technology for MS/MS analysis. The spectra were acquired in the mass range of 700–4000 Da and calibrated internally using the monoisotopic [M + H]<sup>+</sup> ions of trypsin autolytic fragments (842.5 and 2211.1 Da).

Peak lists in XML data format were created using flexAnalysis 3.0 program with SNAP peak detection algorithm. No smoothing was applied and maximal number of assigned peaks was

set to 50. After peak labeling, all known contaminant signals were manually removed. The peak lists were searched using MASCOT search engine against Swiss-Prot 57.6 database subset of human proteins with the following search settings: peptide tolerance of 20 ppm, missed cleavage site value set to two, variable oxidation of methionine and N-acetylation of protein N-terminus. No restriction on protein molecular weight and pI value was applied. Proteins with MOWSE score over the threshold 56 calculated for the used settings were considered as identified. If the score was only slightly higher than the threshold value or the sequence coverage too low, the identity of protein candidate was confirmed by MS/MS analysis. In addition to the above-mentioned MASCOT settings, fragment mass tolerance of 0.6 Da and Ultraflex III instrument (Bruker Daltonics, Bremen, Germany) equipped with a Smartbeam solid state laser and LIFT technology for MS/MS analysis was applied for MS/MS spectra searching.

**The Protein Expression Analysis Using Immunoblot.** The whole-cell lysates prepared as described above were used for SDS-PAGE. For electrophoretic separation of PF 2D fractions, 10% of the total volume of the first-dimension pH fractions was precipitated by trichloroacetic acid, dissolved in 15  $\mu$ L of SDS sample buffer, and loaded on SDS-PAGE.

Following SDS-PAGE using 10, 12, or 15% polyacrylamide gels, separated proteins were transferred onto Immobilon P (Millipore, Bedford, MA) membranes using a semidry blotting system (Biometra, Göttingen, Germany) and transfer buffer containing 48 mM Tris, 39 mM glycine, and 20% methanol.<sup>8</sup> The membranes were blocked in 5% nonfat dry milk or in 5% BSA in Tris-buffered saline with 0.05% Tween 20 (TBST) pH 7.4 for 1 h and incubated overnight with the respective primary antibodies: anti-Rho-GDI2 (Rho GDP-dissociation inhibitor 2; Abcam ab13925; 1:500 in 5% BSA/TBST), anti-YB1 (Y-box binding protein 1; Abcam ab12148; 1:10 000 in 5% nonfat dry milk/TBST), anti-Hop (HSP 70/90 organizing protein; Abcam ab37752; 1:10 000 in 5% nonfat dry milk/TBST), or anti- $\beta$ -tubulin (Sigma T4026; 1:1000 in 5% nonfat dry milk/TBST). Peroxidase-conjugated secondary anti-mouse and anti-rabbit IgG antibodies (Jackson ImmunoResearch, Suffolk, U.K.) were diluted 1:10 000, and anti-chicken IgY (Abcam ab6753) was diluted 1:100 000 in 5% nonfat dry milk/TBST and applied as appropriate. The ECL+ chemiluminescence (GE Healthcare, Uppsala, Sweden) detection system was used to detect specific proteins. The exposed CL-XPosure films (Thermo Scientific, Rockford, IL) were scanned by a calibrated densitometer GS-800 (Bio-Rad, Hercules, CA).

**Protein Expression Profiles Characterized by Immunohistochemistry.** Paraffin-embedded samples of CEM cells, CEM cells treated with 60  $\mu$ M CDKI bohemine for 6 h, CEM-BOH cells resistant to CDKI bohemine, and CEM-BOH cells resistant to CDKI bohemine treated with 60  $\mu$ M CDKI bohemine for 6 h were cut in the sections, mounted on silane-coated slides, deparaffinized, rehydrated, and pretreated in a microwave at 650 W for 30 min in citrate buffer pH 6.0. Nonspecific binding was blocked with 5% rabbit serum in phosphate buffer solution. Sections were incubated in the primary anti-Hop antibody (Abcam ab37752; 1:500). As a secondary antibody, anti-chicken IgY (Abcam ab6753) was applied for 60 min (working dilution 1:400) followed by biotin–streptavidin–peroxidase complex (Dako, Copenhagen, Denmark). Diaminobenzidine substrate was used as a chromogen, according to the manufacturer's instructions (DAKO, Copenhagen, Denmark). Sections were counterstained with hematoxylin.

**Computer Modeling of Protein Interaction Network.** Interologous Interaction Database (I2D; an online database of known and predicted mammalian and eukaryotic protein–protein interactions) was used to search for possible protein–protein interaction partners for proteins identified as regulated during the development of acquired resistance to cyclin-dependent kinases inhibitor. Version 1.8 of I2D, including 254 588 source interactions and 238 553 predicted interactions (<http://ophid.utoronto.ca/ophidv2.201/ppi.jsp>) was used for interaction search with human selected as target organism. Protein–protein interaction network was visualized using NAViGaTOR (Network Analysis, Visualization & Graphing TORonto) software (<http://ophid.utoronto.ca/navigator>). In protein–protein interaction networks, nodes represent proteins and edges between nodes represent physical interactions between the proteins. NAViGaTOR allows nodes to be color-coded according to Gene Ontology (GO, a controlled vocabulary describing properties of genes) terms.

## Results

**Proteomic Changes Observed in CEM-BOH Cells Resistant to CDKI Bohemine Compared to Sensitive CEM Cells Using 2-D LC.** The primary aim of our study was to identify differences in protein expression between CEM-BOH cells resistant to CDKI bohemine and bohemine-sensitive parental CEM cells. The lysates of cell samples were fractionated using 2-D liquid chromatography, resulting proteome maps were evaluated for differentially expressed protein peaks, and identity of the proteins was determined by mass spectrometry. Selected protein changes were verified using immunoblotting and immunohistochemistry. The proteins were further validated for their roles in drug resistance using CEM and A549 cell lines resistant to vincristine or daunorubicin (Figure 1).

The purpose of 2-D LC protein separation performed on PF 2D was to use an advanced gel-independent fractionation technique. This method has the distinct advantage over the 2-DE based approach in that it overcomes many of its drawbacks and, importantly, the fractions of intact proteins can be directly utilized for mass spectrometric analysis. The PF 2D involves 2-D separation and mapping of the total protein expression. Proteins are fractionated by isoelectric points in pH gradient using the chromatofocusing at 0.3 pH intervals in the first dimension. Each of these pH protein fractions is further separated by hydrophobicity using reversed phase in the second dimension.<sup>9</sup> The global information about protein expression obtained by means of PF 2D separation has been depicted using ProteoVue software that enables the construction of 2-D protein map showing pH fractions versus protein hydrophobicity. Reproducibility of the 2-D LC fractionation can be expressed by coefficient of variation which may be calculated using the values of retention time of all peaks, peak heights, or peak areas from several runs as exemplified in the study of Linke et al.<sup>10</sup> While the values of % of coefficient of variation (% CV) are usually low (in average 0.40) for peak retention time, they are obviously higher (around 20) for peak height or peak area. In our study, median % CV based on the values of normalized peak areas was 31. Coefficient of determination  $R^2$  calculated for variations in peak areas between biological replicates was equal to 94% and 96% for protein patterns corresponding to CEM and CEM-BOH cells, respectively, indicating good reproducibility of separation and quantification methods.

In total, 15 fractions collected in the pH range of 8.30–4.10 and one fraction collected in the pH > 8.30 (proteins that did not bind to the HPCF column) were then separated on HPRP column (Figure 2). The 2-D protein maps of all runs performed in this study are shown in Supplemental Figure 1. The samples of CEM and CEM-BOH cells were separated in average into 1229 protein peaks and the evaluation of qualitative and quantitative differences by UV measurement between 2-D protein maps using Viper software identified 6 differentially expressed protein peaks with  $p$ -value  $\leq 0.05$  (Peak Nos: 163, 200, 365, 649, 800, 889) and 12 protein peaks with fold change  $\geq 1.6$  (Peak Nos: 88, 115, 163, 200, 362, 648, 649, 701, 770, 780, 847 and 1145) between sensitive CEM and resistant CEM-BOH cells. Nine of the differentially expressed protein peaks revealed by PF 2D approach were present at decreased level in resistant CEM-BOH cells. On the contrary, six protein bands were found in higher level in resistant CEM-BOH cells (Table 1). Relative differences in expression ranged from 1.6-fold to as much as 8.7-fold. Figure 3 demonstrates an example of differences found in fraction of pH 7.7–8.0 and other differences mentioned

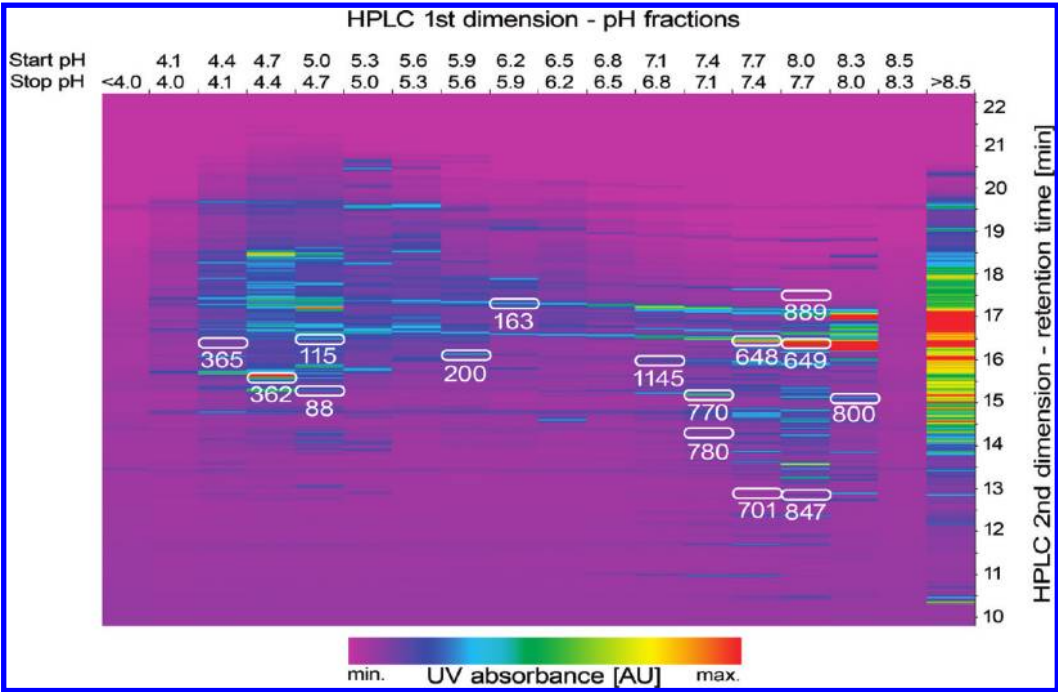


**Figure 2.** Two-dimensional liquid chromatography protein map of CEM cell line and set of protein peaks significantly different in resistant CEM-BOH cells compared to CEM cells. Lysates of cell samples were subjected to 2-D liquid chromatography and protein fractionation was monitored using UV detection. 2-D protein expression maps were generated by ProteoVue software and their images were evaluated using Viper software. Figure shows representative protein map from parental sensitive CEM cells and a set of protein bands significantly different in resistant CEM-BOH cells. The colors of the protein bands correspond to UV intensity and provide information about protein quantification. Regulated protein peaks are indicated by their numbers assigned by Viper software.

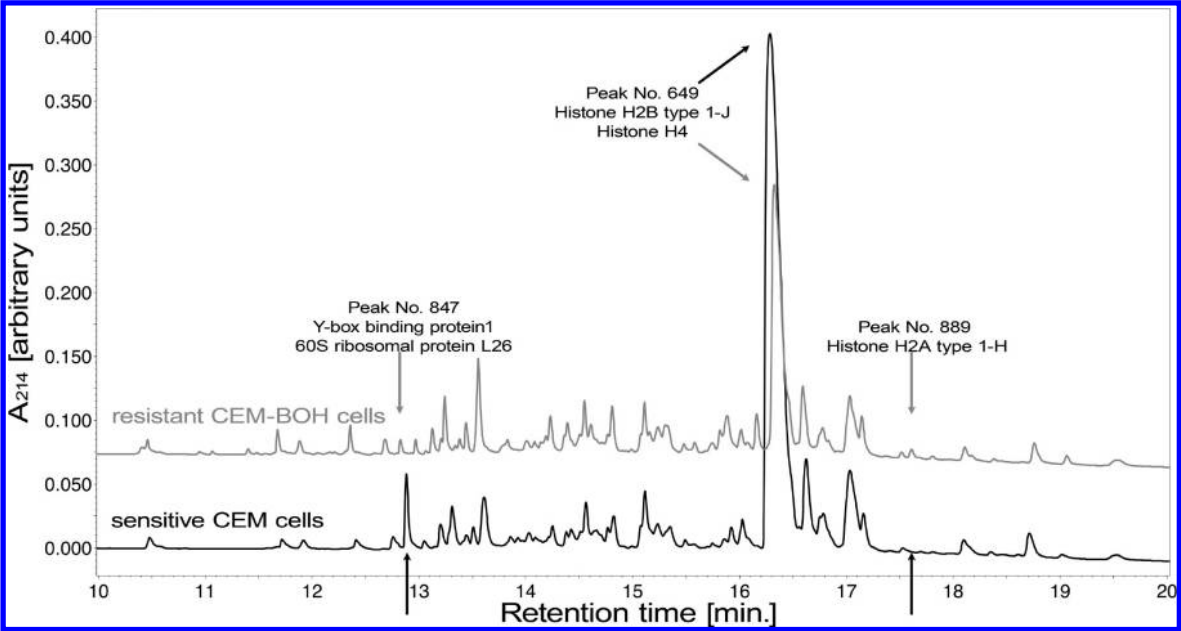


**Figure 3.** The UV profile of second dimension of 2-D HPLC ProteomeLabPF 2D chromatography and comparison of differences between analyzed samples. The UV chromatogram of pH fraction 7.7–8.0 separated in the second dimension on reversed phase column packed with C18 nonporous silica beads. The UV absorptions were monitored at 214 nm. Three protein peaks were found differentially expressed between sensitive CEM cells and CEM-BOH cells resistant to CDKI bohemeine.

above are provided in Supplemental Figure 2). All these discriminate protein peaks were chosen for further mass spectrometry and the proteins in all of them were satisfactorily identified (Table 1). Supplementary Table 1 provides comprehensive information about the proteins (fraction numbers, protein names, database accession numbers, protein MW and pI, and all MS identification data including Mascot scores,

sequence coverage, matched peaks, unmatched peaks, and MS/MS confirmation). Among the proteins identified in differentially regulated protein peaks in resistant CEM-BOH cells were several ribosomal proteins including the proteins of large 60S ribosomal subunit (proteins L4, L6, L7a, L15 and L26) as well as the proteins of the small 40S ribosomal subunit (S4\_X isoform, S8, S13, S24, S25). Furthermore, we have detected



several histone variants, namely, histone H2A type 1-H, histone H2B type 1-B, histone H2B type 1-D, histone H2B type 1-J, and histone H4, to be differently expressed between susceptible and resistant cells. On the basis of our MS data (Supplemental Table 1), we have unambiguously distinguished ribosomal proteins according to the unique peptides that were observed for each identified protein. The only ambiguity in protein identification could be related to specific histone variants within a single core histone, namely, histone H2A and H2B where the top position with the highest score in the protein candidate list given by MASCOT was accepted without any other sequential confirmation. Nevertheless, the core histones H2A, H2B, and H4 were satisfactorily distinguished, and in our opinion, sufficient for the purpose of this study.

It was evident that many of the protein peaks collected after the second dimension contained more than one protein and this was reconfirmed by mass spectrometric analysis. However, there were also protein peaks fulfilling the criteria of one protein/one peak in a fraction: the protein peaks nos. 088 and 701 showing decrease in resistant CEM-BOH cells which corresponded to tubulin-specific chaperone A and Y-box binding protein 1; the protein peaks nos. 362 and 889 showing increase in resistant CEM-BOH cells corresponded to Rho GDP-dissociation inhibitor 2 and histone H2A type 1-H (Table 1, Figure 2).

In the subsequent work, we focused on detailed verification of the proteins (a) with highly elevated/significant increase in resistant CEM-BOH cells: Rho-GDP-dissociation inhibitor 2 (Rho GDI2) with 2.36-fold change and Hsp70/90 organizing protein (Hop; stress-induced phosphoprotein 1- STIP 1) reaching 8.18-fold change; (b) Y-box binding protein 1 (YB-1; nuclease sensitive element-binding protein 1) decreased to almost 9-fold in resistant cells.

**Immunoblotting Verification of Protein Changes Typical for Resistant CEM-BOH Cells.** To validate the results of the proteomic analysis, immunoblot experiments were performed to confirm the identity of the proteins Rho GDI2 and YB-1 which were increased and decreased, respectively, in resistant CEM-BOH cells compared to sensitive CEM cells on PF 2D chromatography. Furthermore, Hop protein identified as one of two unambiguously identified proteins in peak no. 200 from PF 2D with observed higher UV absorbance level in CEM-BOH cells was selected to demonstrate verification and contribution of a particular protein to UV absorbance level corresponding to protein amount.

First, monitoring of protein changes at the level of whole cell lysates was performed. The samples of untreated sensitive CEM and resistant CEM-BOH cells were completed by the cells treated with 60  $\mu$ M CDKI bohemine for 6 h to monitor early response of sensitive as well as resistant cells to the drug that precedes onset of apoptosis. The results shown in Figure 4A confirmed significantly higher level of Rho GDI2 in resistant cells. The treatment by CDKI bohemine resulted in almost undetectable Rho GDI2 level in sensitive cells while in resistant cells showed high Rho GDI2 level. The level of YB-1 protein observed at 50 kDa corresponding to intact protein<sup>11</sup> did not reveal significant difference between the sensitive and resistant cells. In spite of this, similarly to Rho GDI2, treatment by CDKI bohemine resulted in decreased level of YB-1 in sensitive cells but not in resistant cells. The faint protein band observed at 32 kDa represented truncated form of the YB-1 protein<sup>12</sup> which appeared to be more evident in resistant CEM-BOH cells.

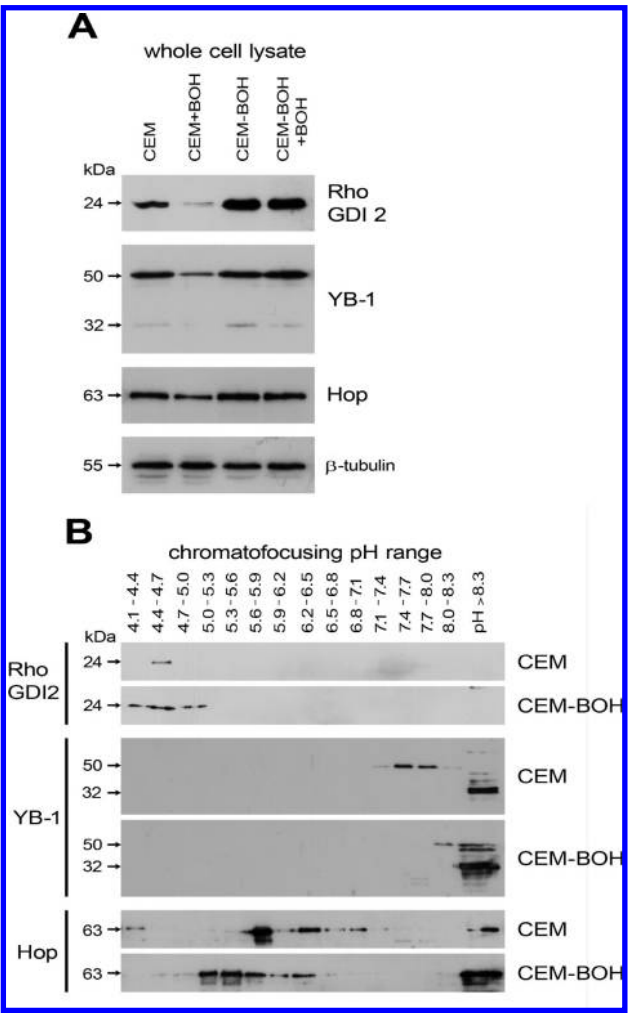


**Figure 4.** Immunoblot analysis of Rho GDP-dissociation inhibitor 2, Hsp70/90 organizing protein, and Y-box binding protein 1 in susceptible CEM cell line and CEM-BOH cells resistant to cyclin-dependent kinases inhibitor bohemine. (A) The whole-cell lysates were prepared from untreated sensitive CEM cell line and CEM-BOH cells resistant to cyclin-dependent kinases inhibitor bohemine (BOH). The samples of untreated cells were completed by the cells exposed by 60  $\mu$ M CDKI bohemine: CEM+BOH and CEM-BOH +BOH. The lysates were examined on immunoblots using specific antibodies recognizing Rho GDP-dissociation inhibitor 2 (Rho GDI2), Hsp70/90 organizing protein (Hop), and Y-box binding protein 1 (YB-1). The  $\beta$ -tubulin was used as a loading control. (B) The pH fractions of the first dimension of 2-D fractionation were analyzed using Western blot to detect changes in specific isoforms of these three selected proteins. The shift in pH of YB-1 and Hop proteins between sensitive CEM cells and resistant CEM-BOH cells was detected.

Additionally, the total level of Hop did not reveal significant difference between the sensitive and resistant cells.

Second, protein changes were verified directly in pH fractions from PF 2D in order to look whether different protein forms/variants contribute to the observed alterations (Figure 4B). In case of Rho GDI2, immunoblot of PF 2D pH fractions confirmed massive elevation of the level in resistant cells with spread over several fractions that were symmetrically distributed around protein pH observed in sensitive cells. On the contrary, immunoblot of pH fractions confirmed the presence of acidic 50 kDa YB-1 protein forms (pH 7.1–8.0) in sensitive cells which were not observed in resistant cells. In resistant



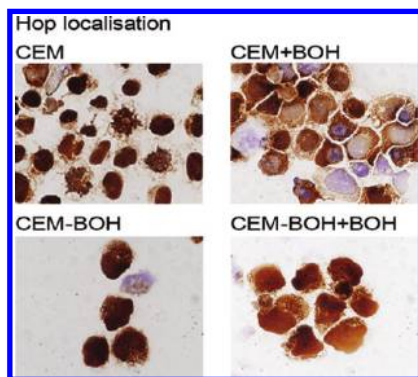


**Figure 5.** Subcellular localization of Hsp70/90 organizing protein in susceptible CEM cell line and CEM-BOH cells resistant to cyclin-dependent kinases inhibitor bohemin. Untreated sensitive CEM cell line, CEM-BOH cells resistant to cyclin-dependent kinases inhibitor bohemin (BOH), and both cell lines exposed by 60  $\mu$ M CDKI bohemin: CEM+BOH and CEM-BOH+BOH were analyzed using immunohistochemistry (magnification 800 $\times$ ). Translocation of Hop from nuclei to cytoplasm was observed in sensitive CEM cells after treatment with bohemin. In resistant cells, the Hop protein was localized both in nuclei and cytoplasm and the treatment had no effect on protein level/localization.

cells, both protein forms at 50 and 32 kDa were found only in basic fraction with pH higher than 8.3. We could also observe the shift of Hop protein which was distributed in more acidic pH at 5.0–5.6 in resistant cells compared to its predominance at around pH 6.0 in susceptible counterparts. It is likely that the more acidic forms of Hop in CEM-BOH cells represent phosphorylated protein.<sup>13</sup>

**Different Subcellular Distribution of the Hop Protein in Resistant CEM-BOH Cells.** With respect to the published observations that phosphorylation of Hop protein has impact on its cellular functions as well as localization,<sup>14,15</sup> we used immunohistochemistry to study distribution of Hop protein in sensitive CEM and resistant CEM-BOH cells. As in the in above-mentioned immunoblot experiments, the samples of untreated sensitive CEM and resistant CEM-BOH cells were completed by the cells treated with 60  $\mu$ M CDKI bohemin for 6 h.

The staining of the Hop protein was high in the nuclei of sensitive CEM cells and appeared to be closely associated to chromosomes. In comparison to this picture, the protein in resistant CEM-BOH cells was localized in both nuclei and cytoplasm. Treatment by CDKI bohemin resulted in decreased staining of Hop protein in nuclei and partial translocation to the cytoplasm in sensitive cells but did not evidently influence the expression pattern in resistant cells (Figure 5).

**The Level of Rho GDI2, YB-1, and Hop Proteins in CEM and A549 Cell Lines Resistant to Bohemin, Vincristine, or Daunorubicin.** To study the Rho GDI2, YB-1, and Hop proteins for their role in drug resistance, we further examined CEM cell lines resistant to vincristine (CEM-VCR) or daunorubicin (CEM-DNR) as well as representatives of solid tumor, lung adenocarcinoma cell lines A549 resistant to CDKI bohemin (A549-BOH) or vincristine (A549-VCR). Among conventional chemotherapeutic drugs, vincristine belongs to microtubule dynamics affecting drug and daunorubicin is DNA damaging agent. The resistant cell lines were derived and characterized previously.<sup>7</sup>

The immunoblot of whole-cell lysates confirmed increase in the level of Rho GDI2 in all resistant cell lines, including CEM-VCR and CEM-DNR cells compared to parental CEM cells and

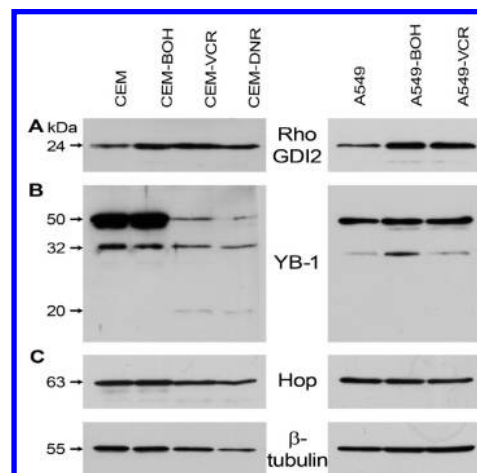


**Figure 6.** The level of Rho-GDP-dissociation inhibitor 2, Hsp70/90 organizing protein, and Y-box binding protein 1 in cell lines resistant to vincristine or daunorubicin. The samples of CEM cell lines resistant to vincristine (CEM-VCR) or daunorubicin (CEM-DNR) as well as A549 cell lines resistant to CDKI bohemin (A549-BOH) or vincristine (A549-VCR) were examined on immunoblots using specific antibodies recognizing Rho-GDP-dissociation inhibitor 2 (A), Y-box binding protein 1 (B), and Hsp70/90 organizing protein (C). The  $\beta$ -tubulin was used as a loading control.

A549-VCR or A549-DNR cells compared to parental A549 cells (Figure 6A). The expression of YB-1 protein observed in both CEM and CEM-BOH cells at the 50 and 32 kDa bands was without any evident changes between sensitive and resistant cells. On the contrary, the full-length YB-1 protein band at 50 kDa was almost diminished in CEM-VCR and CEM-DNR cells and, in addition to observed 32 kDa truncated form, the appearance of 20 kDa cleaved isoform was evident. Furthermore, the presence of a 32 kDa band of truncated YB-1 protein was also typical for A549-BOH resistant cell line (Figure 6B). The total level of Hop was not different among sensitive cells and cells resistant to bohemin, vincristine, or daunorubicin (Figure 6C); however, it does not exclude the role of specific protein form or its post-translational modification in resistant cells as evidenced by 2-D fractionation mentioned above.

**Computer Modeling and Simulation of Possible Interaction Network Connecting Potential Candidate Proteins Regulated during the Development of Acquired Resistance to CDKI.** Identified proteins differentially regulated during the development of acquired resistance to cyclin-dependent kinases inhibitor (Protein/Swiss-Prot accession numbers provided in Table 1) were introduced into I2D database in order to identify possible interaction partners and to construct a protein–protein interaction network that enables to graphically visualize possible functional relationships among identified molecules (Figure 7). The network exposed many additional interaction proteins with a role in the development of acquired resistance to anti-cancer drugs. In total, 2060 interactions were recognized for the 26 proteins identified in this study (Supplemental Table 2). Computer modeling highlighted a high number of direct as well as mediated interactions among ribosomal proteins, histones, and elongation factor 1- $\alpha$  1, thus, networking transcriptional and translational pathways. Furthermore, it was of interest to observe interconnection of the YB-1 and Hop proteins with this network, namely, direct interaction of Hop protein with elongation factor 1- $\alpha$  1 and link between YB-1 and Hop proteins mediated by three interacting proteins:

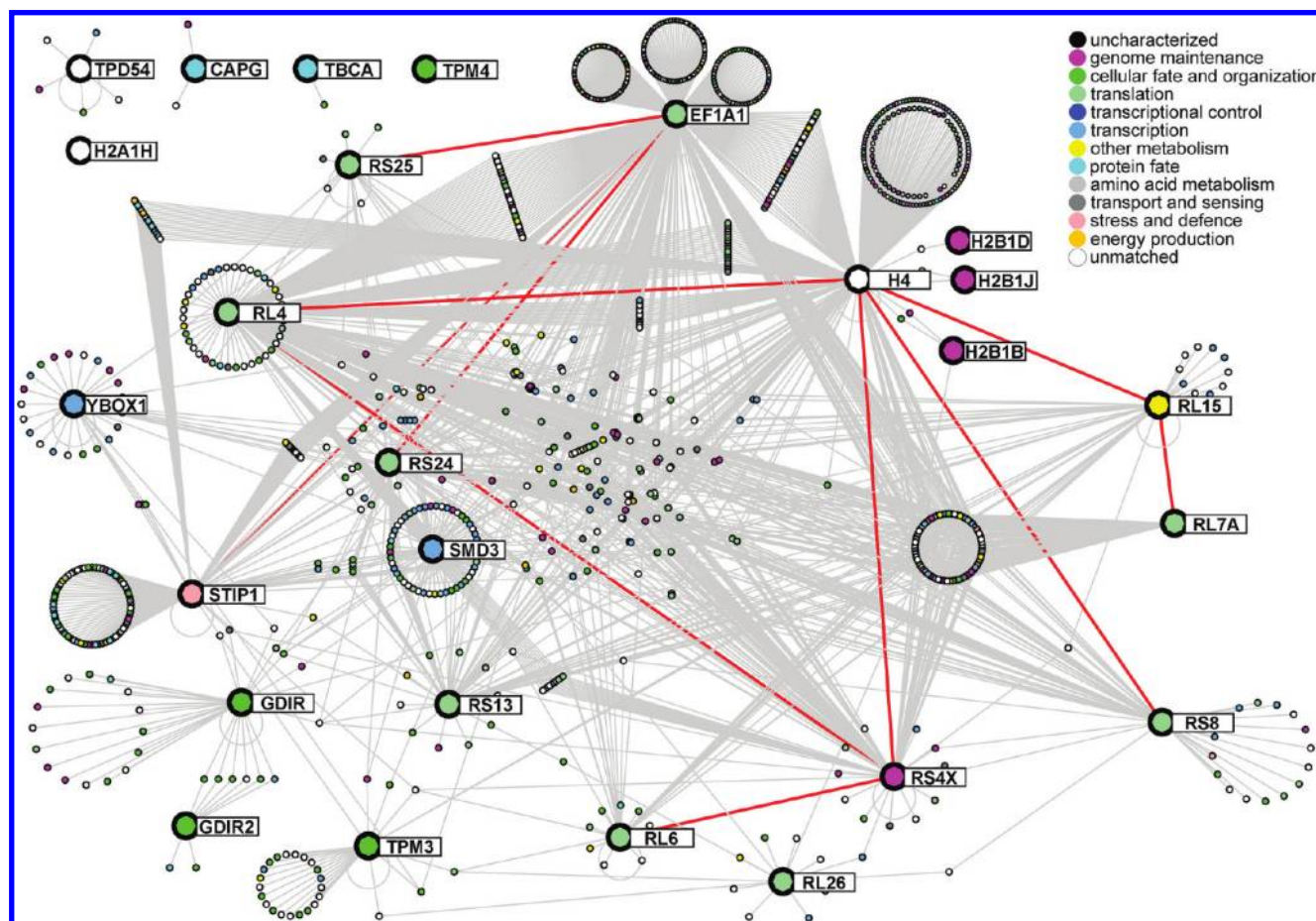


**Figure 7.** Computer modeling and simulation of possible interaction network connecting potential candidate proteins regulated during the development of acquired anti-cancer drug resistance. Network of possible protein–protein interactions, generated by querying I2D database and NAViGaTOR software for 26 identified proteins which were found to be regulated during the development of acquired anti-cancer drug resistance. Some interacting proteins, with direct interconnection are highlighted by red link. Color of nodes and edges represents Gene Ontology function.

Cullin-1 (CUL1; UniProt Q13616), Glycogen synthase kinase-3 beta (GSK3B; UniProt ID P49841), and S-phase kinase-associated protein 1 (SKP1A; UniProt P63208). Contrary to the above, the Rho GDI2 remains to be segregated from this interaction network.

## Discussion

Resistance to anti-cancer drugs is a well-recognized problem and very often it is responsible for failure of the cancer treatment. Unfortunately, drug resistance has been observed not only to conventional chemotherapy but also to molecularly targeted anti-cancer drugs.<sup>2</sup> In our studies we considered selective cyclin-dependent kinases inhibitor as a promising anti-cancer drug. To date, some derivatives of this group of anti-cancer agents have been subjected to pilot clinical trials. Despite this, there are expectations of high probability of resistance development toward this type of selective drugs which may significantly contribute to failure of therapy.

Proteomic analyses of model cancer cell lines have been focused on molecular mechanisms of resistance to many different conventional anti-cancer chemotherapeutic drugs with the primary aim of identifying potential targets of resistance within the cell that would help in selective elimination of specific resistant cell types in actual disease state. The data published to date demonstrated a variety of protein alterations

in drug-resistant cells that could contribute to resistance development.<sup>2,16</sup> The protein fractionation using 2-DE was most frequently applied in those experiments. Hence, many of the proteins on the list were relatively highly abundant proteins. Typically, it is exemplified by observed up-regulated expressions of HSP27, 14-3-3 $\sigma$ , and peroxiredoxins which are on the published list of the top 15 most often identified differentially expressed proteins/protein families in proteomics, regardless of the type of experiments, tissue, and even species.<sup>17</sup> The interpretation of such proteomic data has to be very carefully evaluated as regards specificity of these protein changes and before they are considered as relevant in a particular biological model. Hence, selection of the potential candidate proteins that may have crucial roles in molecular mechanisms of drug-resistance and verification using other independent techniques is critical and necessary. The advantage of the above-mentioned list of the top 15 proteins as suggested by Petrak et al.<sup>17</sup> is the possibility of short-listing of differentially expressed candidate proteins to access the more relevant potential drug targets.

To track down more specific proteins contributing to the development of resistance to CDKI, we used advanced gel-independent liquid-phase 2-D HPLC protein fractionation system that enabled in-depth study for selection of the key potential drug targets. We have used CEM T-lymphoblastic

leukemia cells, which are chemosensitive to a majority of anti-cancer drugs except for the glucocorticoids, and are frequently used for preparation and functional studies of drug resistant sublines.<sup>7</sup> Interestingly, although CEM cells have heterozygous mutations at codons 175/248 (175His/248His) of the p53 gene, the mutated protein forms complexes with DNA leading to transactivation and thus keeping pathway p53 functional.<sup>18</sup> In total, we have identified 26 protein species in 15 differentially expressed protein peaks between sensitive and resistant cells. A majority of the protein changes, in contrast to the previously published 2-DE-based studies, were found to belong to the ribosomal proteins and histones indicating deregulation of translational and transcriptional pathways, respectively, as well as possible epigenetic regulation. The results from our previous study showed down-regulation of three histone variants with different pI and hydrophobicity in response to CDKI bohemine, demonstrating that anti-mitotic and anti-cancer activities of this compound may be associated with epigenetic regulation at the level of chromatin structure.<sup>9</sup> In the study presented here, these activities involved in primary response to CDKI bohemine also contribute significantly to acquired resistance to anti-cancer drug.

Taking into consideration values of fold change and/or significance of the observed differences, it appeared evident that the best potential drug targets could be found among the proteins Rho GDI2, Hop and YB-1. As measured at the total protein levels, only the Rho GDI2 confirmed observed proteome data indicating increased level in resistant CEM-BOH cells. Despite this observation, sensitive CEM cells responded to CDKI bohemine treatment by decrease in the levels of all three candidate proteins, Rho GDI2, YB-1, and Hop, while their protein levels did not change after the treatment in CEM-BOH resistant cells. More detailed immunoblot verification after 2-D separation of cellular proteins clearly demonstrated that, in case of Hop and YB-1 proteins, the observed changes corresponded more to the presence of different protein forms or variants or modifications between susceptible and resistant cells. These findings have subsequently led us to hypothesize that up-regulation of Rho GDI2 level together with the presence of more basic YB-1 protein forms and more acidic Hop variants can make CEM cells less vulnerable to anti-cancer inhibitors of CDKs.

The Rho GDI2 belongs to a family of the GDP dissociation inhibitors, which are pivotal regulators of small GTPases, including Ras1, Cdc42, and RhoA. It was shown to be preferentially expressed in hematopoietic tissues and in B- and T-cell lines and its expression in bladder,<sup>19–21</sup> ovarian,<sup>22</sup> and breast cancer cells<sup>23,24</sup> has been demonstrated by various researchers. Some such published studies have attempted to relate the expression of this particular protein to the invasiveness or metastatic potential within different types of tumors with resultant controversy, indicating that RhoGDI2 may act differently in progression of different tumors.<sup>19,21,24–26</sup> More acceptable and clearly evident seems to be the link between increased RhoGDI2 expression and anti-cancer drug resistance in several cancer cell types.<sup>27</sup> In relation to these findings on Rho GDI2 and its overexpression in ovarian cancer resistant to paclitaxel or in fibrosarcoma cell line resistant to mitoxantrone,<sup>27,28</sup> our study shows that Rho GDI2 protein level is induced in leukemia CEM cells and lung adenocarcinoma A549 cells resistant to CDKI bohemine, vincristine, and daunorubicin. The mechanism by which overexpressed Rho GDI2 could most likely contribute to drug resistance would be due to an anti-apoptotic effect. This is

supported by the fact that Rho GDIs form complexes with Rho, Ras or Cdc42, Rho GDI2 thereby blocking the apoptotic signal pathway mediated by Ras and c-Jun kinases.<sup>27</sup> Rho GDI2 thus represents a very promising potential marker of resistance to several different cytostatic drugs by various cancers. Such a multidrug resistance marker could be crucial in the determination of drug regimens for patients undergoing cytostatic chemotherapy and may have a significant bearing on the final outcome.

The YB-1 protein, which is the member of the cold shock domain protein family, has several pleiotropic functions in the regulation of gene transcription and translation, DNA repair, and cellular responses to environmental stimuli.<sup>29</sup> YB-1 activity and subcellular distribution may be regulated by its phosphorylation<sup>11</sup> and its proteolysis mediated by proteasome cleavage.<sup>12</sup> Sutherland et al.<sup>30</sup> showed that phosphorylation by Akt kinase may induce nuclear translocation of YB-1. Furthermore, the YB-1 protein is transcriptionally activated via newly discovered transcriptional factor Twist, which also directly transactivates Akt2 gene in T-cell leukemias.<sup>31</sup> Akt2 kinase survival pathway is associated with chemoresistance against multiple cytotoxic and targeted therapies. The studies of truncated YB-1 forms revealed that its localization in nuclei of human cancers including breast, ovarian, prostate, colon, osteosarcoma, and synovial sarcoma could be a marker for poor patient outcome and multiple drug resistance.<sup>12,29,32–34</sup> We detected truncated form of YB-1 in leukemia CEM cells resistant to CDKI bohemine, vincristine, and daunorubicin and in lung adenocarcinoma A549 cells resistant to CDKI bohemine. This profile is in agreement with involvement of proteolytic cleavage of YB-1 form in multidrug resistance. Furthermore, our study showed that the presence of more basic YB-1 form(s) is typical for CEM cell resistant to CDKI. The modifications causing this pH shift may include changes in protein phosphorylations but truncations or deletions cannot be excluded.<sup>35</sup>

Human Hop is a co-chaperone mediating the association of the molecular chaperones Hsp70 and Hsp90.<sup>36</sup> The best characterized function of Hop protein is its participation in steroid receptor signaling including glucocorticoid response (reviewed in Daniel et al.).<sup>37</sup> More recent findings suggest that Hop can not only associate with Hsp70 and 90 and modulate their activities, but also interact with several other proteins as mentioned above as well as the prion proteins.<sup>15,37</sup> There is evidence that murine homologue mSTI and human Hop may be phosphorylated and this modification affects protein localization.<sup>14,38</sup> In our study, the Hop in resistant CEM-BOH cells was more acidic than in parental CEM cells sensitive to CDKI bohemine but resistant to glucocorticoid dexamethasone suggesting that in CEM-BOH resistant cells Hop may undergo enhanced phosphorylation. Further findings from immunohistochemistry revealed that Hop is localized in nucleus as well as cytoplasm in CEM-BOH resistant cells in contrast to its prevailing accumulation in nucleus in CEM cells. Hence, the shift to more acidic forms appears to be associated with protein translocation to cytoplasm and development of resistance of CEM cells to anti-cancer CDKI bohemine. Interestingly, Longshaw et al.<sup>14</sup> showed that inhibition of cdc2 kinase triggered by CDKI olomoucine, belonging to the same group of anti-cancer compounds as bohemine, resulted in the nuclear accumulation of mSTI in mouse fibroblasts. On the basis of our findings, it is possible to hypothesize that Hop shuttling induced by CDKI bohemine and associated with development of resistance to this drug in CEM cells which are also resistant



to glucocorticoids may influence steroid receptor signaling via modulation of expression and/or post-translational modification of Hop co-chaperone.

Cancer, the world's second largest killer, has the highest need for new innovative treatments to increase the numbers of patients cured, and to decrease chemoresistant failures resulting in mortality. Drug resistance to synthetic CDK inhibitors is a poorly understood phenomenon and our results demonstrate that, unlike with other anti-cancer drugs, trisubstituted purine analogues represented by bohemine and roscovitine do not induce expression of multidrug resistance proteins. Moreover, roscovitine showed higher efficacy in P-glycoprotein overexpressing cells<sup>39</sup> highlighting these small molecules for therapy of multidrug resistant cancers. Collectively, our study has revealed that Y-box binding protein 1 and the HSP70/90 organizing protein have a critical role to play and interact with the protein nodes of transcriptional and translational networks that are also regulated by CDKI bohemine during the development of acquired resistance to this anti-cancer drug. To add to this, another important role may also be assigned to the Rho-GDP-dissociation inhibitor 2 due to an anti-apoptotic effect and potential effect in multidrug resistance.

## Conclusion

While there is plenty of evidence for pre-eminence in basic research on chemoresistance for different cancers, there seems to be a profound lack of translational research (converting basic discoveries into innovative cures) for the benefit of cancer patients. Additionally, cancer related research and treatment costs are spiralling unless action is taken to improve research outcome on chemoresistance which in turn may impact survival rates as well as push down mortality rates. In particular, uptake of novel technologies and lack of specific biomarkers of the disease are proving to be key barriers to improvement. We have endeavored to work with several proteomic technologies and for a quest for proteins as specific biomarkers that may facilitate better and early diagnosis or as a handle for rapidly assessing chemoresistance to single or multidrug treatment.

The results presented in this study indicate that not only qualitative/quantitative protein changes play an important role in drug-resistance, but that there are various other parameters that too, may have a significant influence on the outcome. More importantly, truncation and/or post-translational modification(s) of selected proteins may alter their subcellular localization as well as their key role in controlling response of cancer cells to anti-cancer treatment. Additionally, simulation of possible interaction network could be used to extrapolate both the functional interpretation as well as the validity of such proteomic findings.

Further studies on these identified proteins are needed and may help to resolve many of the discrepancies between drug treatment for various cancers and poor outcome due to chemoresistance to the drugs in cancer medicine.

**Abbreviations:** A549-BOH, human A549 cells resistant to bohemine; A549-VCR, human A549 cells resistant to vincristine; CDKI, inhibitor of cyclin-dependent kinases; CEM-DNR, human CEM cells resistant to daunorubicin; CEM-VCR, human CEM cells resistant to vincristine; Hop, Hsp70/90 organizing protein (stress-induced phosphoprotein 1); HPCF, high-performance chromatofocusing fractionation; HPRP, high-performance reverse phase fractionation; MeCN, acetonitrile; SDS, sodium dodecyl sulfate; Rho GDI2, Rho GDP-dissociation

inhibitor 2; TBST, Tris-buffered saline with 0.05% Tween 20; TFA, trifluoroacetic acid; YB-1, Y-box binding protein 1 (nuclease sensitive element-binding protein 1).

**Acknowledgment.** This study was supported by the Czech Ministry of School and Education (grant number LC07017) and Institutional Research Concepts AV0Z50450515 (IAPG AS CR,v.v.i.) and AV0Z50200510 (IMIC AS CR, v.v.i.), Grant Agency of the Czech Republic GACR 301/08/1649. Infrastructural part of this project (Institute of Molecular and Translational Medicine) was supported from the Operational Program Research and Development for Innovations (project CZ.1.05/2.1.00/01.0030).

**Supporting Information Available:** Supplemental Figure 1, 2-D liquid chromatography protein maps of sensitive CEM and resistant CEM-BOH cells; Supplemental Figure 2, the UV profiles of the second dimension HPRP fractionations of pH fractions with significant UV differences in protein peaks found between sensitive CEM cells and resistant CEM-BOH counterparts; Supplemental Table 1, table of differentially expressed proteins identified in 2-D HPLC experiment including mass spectrometry data; Supplemental Table 2, I2D protein-protein Interaction search results. This material is available free of charge via the Internet at <http://pubs.acs.org>.

## References

- (1) Raguz, S.; Yague, E. Resistance to chemotherapy: new treatments and novel insights into an old problem. *Br. J. Cancer* **2008**, *99* (3), 387–91.
- (2) Zhang, J. T.; Liu, Y. Use of comparative proteomics to identify potential resistance mechanisms in cancer treatment. *Cancer Treat. Rev.* **2007**, *33* (8), 741–56.
- (3) Dean, M.; Fojo, T.; Bates, S. Tumour stem cells and drug resistance. *Nat. Rev. Cancer* **2005**, *5* (4), 275–84.
- (4) Hajdich, M., Skalnikova, H., Halada, P., Vydra, D., Dzubak, P., Dziechciarkova, M., Strnad, M., Radioch, D., Kovarova, H., Cyclin-dependent kinase inhibitors and cancer: usefulness of proteomic approaches in assessment of the molecular mechanisms and efficacy of novel therapeutics. In *Clinical Proteomics: From Diagnosis to Therapy*; Van Eyk, J. E., Dunn, M. J., Eds.; Wiley-VCH: Weinheim, 2007; pp 177–202.
- (5) Kovarova, H.; Hajdich, M.; Korinkova, G.; Halada, P.; Krupickova, S.; Gouldsworthy, A.; Zhelev, N.; Strnad, M. Proteomics approach in classifying the biochemical basis of the anticancer activity of the new olomoucine-derived synthetic cyclin-dependent kinase inhibitor, bohemine. *Electrophoresis* **2000**, *21* (17), 3757–64.
- (6) Dobashi, Y.; Takehana, T.; Ooi, A. Perspectives on cancer therapy: cell cycle blockers and perturbators. *Curr. Med. Chem.* **2003**, *10* (23), 2549–58.
- (7) Noskova, V.; Dzubak, P.; Kuzmina, G.; Ludkova, A.; Stehlik, D.; Trojanec, R.; Janostakova, A.; Korinkova, G.; Mihal, V.; Hajdich, M. In vitro chemoresistance profile and expression/function of MDR associated proteins in resistant cell lines derived from CCRF-CEM, K562, A549 and MDA MB 231 parental cells. *Neoplasma* **2002**, *49* (6), 418–25.
- (8) Towbin, H.; Staehelin, T.; Gordon, J. Electrophoretic transfer of proteins from polyacrylamide gels to nitrocellulose sheets: procedure and some applications. *Proc. Natl. Acad. Sci. U.S.A.* **1979**, *76* (9), 4350–4.
- (9) Skalnikova, H.; Halada, P.; Dzubak, P.; Hajdich, M.; Kovarova, H. Protein fingerprints of anti-cancer effects of cyclin-dependent kinase inhibition: identification of candidate biomarkers using 2-D liquid phase separation coupled to mass spectrometry. *Technol. Cancer Res. Treat.* **2005**, *4* (4), 447–54.
- (10) Linke, T.; Ross, A. C.; Harrison, E. H. Proteomic analysis of rat plasma by two-dimensional liquid chromatography and matrix-assisted laser desorption ionization time-of-flight mass spectrometry. *J. Chromatogr., A* **2006**, *1123* (2), 160–9.
- (11) Bader, A. G. YB-1 activities in oncogenesis: transcription and translation. *Curr. Cancer Ther. Rev.* **2006**, *2* (1), 31–9.
- (12) Sorokin, A. V.; Selyutina, A. A.; Skabkin, M. A.; Guryanov, S. G.; Nazimov, I. V.; Richard, C.; Th'ng, J.; Yau, J.; Sorensen, P. H.; Ovchinnikov, L. P.; Evdokimova, V. Proteasome-mediated cleavage



- of the Y-box-binding protein 1 is linked to DNA-damage stress response. *EMBO J.* **2005**, 24 (20), 3602–12.
- (13) Honore, B.; Leffers, H.; Madsen, P.; Rasmussen, H. H.; Vandekerckhove, J.; Celis, J. E. Molecular cloning and expression of a transformation-sensitive human protein containing the TPR motif and sharing identity to the stress-inducible yeast protein STI1. *J. Biol. Chem.* **1992**, 267 (12), 8485–91.
  - (14) Longshaw, V. M.; Chapple, J. P.; Balda, M. S.; Cheetham, M. E.; Blatch, G. L. Nuclear translocation of the Hsp70/Hsp90 organizing protein mSTI1 is regulated by cell cycle kinases. *J. Cell Sci.* **2004**, 117 (Pt. 5), 701–10.
  - (15) Odunuga, O. O.; Longshaw, V. M.; Blatch, G. L. Hop: more than an Hsp70/Hsp90 adaptor protein. *BioEssays* **2004**, 26 (10), 1058–68.
  - (16) Petrak, J.; Toman, O.; Simonova, T.; Halada, P.; Cmejla, R.; Klenner, P.; Zivny, J. Identification of molecular targets for selective elimination of TRAIL-resistant leukemia cells. From spots to in vitro assays using TOP15 charts. *Proteomics* **2009**, 9 (22), 5006–15.
  - (17) Petrak, J.; Ivanek, R.; Toman, O.; Cmejla, R.; Cmejlova, J.; Vyoral, D.; Zivny, J.; Vulpe, C. D. Deja vu in proteomics. A hit parade of repeatedly identified differentially expressed proteins. *Proteomics* **2008**, 8 (9), 1744–9.
  - (18) Park, D. J.; Nakamura, H.; Chumakov, A. M.; Said, J. W.; Miller, C. W.; Chen, D. L.; Koeffler, H. P. Transactivational and DNA binding abilities of endogenous p53 in p53 mutant cell lines. *Oncogene* **1994**, 9 (7), 1899–906.
  - (19) Gildea, J. J.; Seraj, M. J.; Oxford, G.; Harding, M. A.; Hampton, G. M.; Moskaluk, C. A.; Frierson, H. F.; Conaway, M. R.; Theodorescu, D. RhoGDI2 is an invasion and metastasis suppressor gene in human cancer. *Cancer Res.* **2002**, 62 (22), 6418–23.
  - (20) Seraj, M. J.; Harding, M. A.; Gildea, J. J.; Welch, D. R.; Theodorescu, D. The relationship of BRMS1 and RhoGDI2 gene expression to metastatic potential in lineage related human bladder cancer cell lines. *Clin. Exp. Metastasis* **2000**, 18 (6), 519–25.
  - (21) Theodorescu, D.; Sapinoso, L. M.; Conaway, M. R.; Oxford, G.; Hampton, G. M.; Frierson, H. F., Jr. Reduced expression of metastasis suppressor RhoGDI2 is associated with decreased survival for patients with bladder cancer. *Clin. Cancer Res.* **2004**, 10 (11), 3800–6.
  - (22) Tapper, J.; Kettunen, E.; El-Rifai, W.; Seppala, M.; Andersson, L. C.; Knuutila, S. Changes in gene expression during progression of ovarian carcinoma. *Cancer Genet. Cytogenet.* **2001**, 128 (1), 1–6.
  - (23) Jiang, W. G.; Watkins, G.; Lane, J.; Cunnick, G. H.; Douglas-Jones, A.; Mokbel, K.; Mansel, R. E. Prognostic value of rho GTPases and rho guanine nucleotide dissociation inhibitors in human breast cancers. *Clin. Cancer Res.* **2003**, 9 (17), 6432–40.
  - (24) Schunke, D.; Span, P.; Ronneburg, H.; Dittmer, A.; Vetter, M.; Holzhausen, H. J.; Kantelhardt, E.; Krenkel, S.; Muller, V.; Sweep, F. C.; Thomssen, C.; Dittmer, J. Cyclooxygenase-2 is a target gene of rho GDP dissociation inhibitor beta in breast cancer cells. *Cancer Res.* **2007**, 67 (22), 10694–702.
  - (25) Cho, H. J.; Baek, K. E.; Park, S. M.; Kim, I. K.; Choi, Y. L.; Nam, I. K.; Hwang, E. M.; Park, J. Y.; Han, J. Y.; Kang, S. S.; Kim, D. C.; Lee, W. S.; Lee, M. N.; Oh, G. T.; Kim, J. W.; Lee, C. W.; Yoo, J. RhoGDI2 expression is associated with tumor growth and malignant progression of gastric cancer. *Clin. Cancer Res.* **2009**, 15 (8), 2612–9.
  - (26) Zhao, J.; Chang, A. C.; Li, C.; Shedden, K. A.; Thomas, D. G.; Misk, D. E.; Manoharan, A. P.; Giordano, T. J.; Beer, D. G.; Lubman, D. M. Comparative proteomics analysis of Barrett metaplasia and esophageal adenocarcinoma using two-dimensional liquid mass mapping. *Mol. Cell. Proteomics* **2007**, 6 (6), 987–99.
  - (27) Goto, T.; Takano, M.; Sakamoto, M.; Kondo, A.; Hirata, J.; Kita, T.; Tsuda, H.; Tenjin, Y.; Kikuchi, Y. Gene expression profiles with cDNA microarray reveal RhoGDI as a predictive marker for paclitaxel resistance in ovarian cancers. *Oncol. Rep.* **2006**, 15 (5), 1265–71.
  - (28) Sinha, P.; Hutter, G.; Kottgen, E.; Dietel, M.; Schadendorf, D.; Lage, H. Search for novel proteins involved in the development of chemoresistance in colorectal cancer and fibrosarcoma cells in vitro using two-dimensional electrophoresis, mass spectrometry and microsequencing. *Electrophoresis* **1999**, 20 (14), 2961–9.
  - (29) Kuwano, M.; Oda, Y.; Izumi, H.; Yang, S. J.; Uchiumi, T.; Iwamoto, Y.; Toi, M.; Fujii, T.; Yamana, H.; Kinoshita, H.; Kamura, T.; Tsuneyoshi, M.; Yasumoto, K.; Kohno, K. The role of nuclear Y-box binding protein 1 as a global marker in drug resistance. *Mol. Cancer Ther.* **2004**, 3 (11), 1485–92.
  - (30) Sutherland, B. W.; Kucab, J.; Wu, J.; Lee, C.; Cheang, M. C.; Yorida, E.; Turbin, D.; Dedhar, S.; Nelson, C.; Pollak, M.; Leighton Grimes, H.; Miller, K.; Badve, S.; Huntsman, D.; Blake-Gilks, C.; Chen, M.; Pallen, C. J.; Dunn, S. E. Akt phosphorylates the Y-box binding protein 1 at Ser102 located in the cold shock domain and affects the anchorage-independent growth of breast cancer cells. *Oncogene* **2005**, 24 (26), 4281–92.
  - (31) Tanji, H.; Ishikawa, C.; Sawada, S.; Nakachi, S.; Takamatsu, R.; Matsuda, T.; Okudaira, T.; Uchiyama, J. N.; Ohshiro, K.; Tanaka, Y.; Senba, M.; Uezato, H.; Ohshima, K.; Duc Dodon, M.; Wu, K. J.; Mori, N. Aberrant expression of the transcription factor Twist in adult T-cell leukemia. *Blood* **2010**, 116 (8), 1386.
  - (32) Bargou, R. C.; Jurchott, K.; Wagener, C.; Bergmann, S.; Metzner, S.; Bommert, K.; Mapara, M. Y.; Winzer, K. J.; Dietel, M.; Dorken, B.; Royer, H. D. Nuclear localization and increased levels of transcription factor YB-1 in primary human breast cancers are associated with intrinsic MDR1 gene expression. *Nat. Med.* **1997**, 3 (4), 447–50.
  - (33) Fujita, T.; Ito, K.; Izumi, H.; Kimura, M.; Sano, M.; Nakagomi, H.; Maeno, K.; Hama, Y.; Shingu, K.; Tsuchiya, S.; Kohno, K.; Fujimori, M. Increased nuclear localization of transcription factor Y-box binding protein 1 accompanied by up-regulation of P-glycoprotein in breast cancer pretreated with paclitaxel. *Clin. Cancer Res.* **2005**, 11 (24 Pt. 1), 8837–44.
  - (34) Oda, Y.; Ohishi, Y.; Saito, T.; Hinoshita, E.; Uchiumi, T.; Kinukawa, N.; Iwamoto, Y.; Kohno, K.; Kuwano, M.; Tsuneyoshi, M. Nuclear expression of Y-box-binding protein-1 correlates with P-glycoprotein and topoisomerase II alpha expression, and with poor prognosis in synovial sarcoma. *J. Pathol.* **2003**, 199 (2), 251–8.
  - (35) Zhu, K.; Zhao, J.; Lubman, D. M.; Miller, F. R.; Barder, T. J. Protein pI shifts due to posttranslational modifications in the separation and characterization of proteins. *Anal. Chem.* **2005**, 77 (9), 2745–55.
  - (36) Lassle, M.; Blatch, G. L.; Kundra, V.; Takatori, T.; Zetter, B. R. Stress-inducible, murine protein mSTI1. Characterization of binding domains for heat shock proteins and in vitro phosphorylation by different kinases. *J. Biol. Chem.* **1997**, 272 (3), 1876–84.
  - (37) Daniel, S.; Soti, C.; Csermely, P.; Bradley, G.; Blatch, G. L. Hop: An Hsp70/Hsp90 co-chaperone that functions within and beyond Hsp70/Hsp90 protein folding pathways. In *Networking of Chaperones by Co-Chaperones*; Blatch, G. L., Ed.; Springer: New York, 2007; pp 26–37.
  - (38) Daniel, S.; Bradley, G.; Longshaw, V. M.; Soti, C.; Csermely, P.; Blatch, G. L. Nuclear translocation of the phosphoprotein Hop (Hsp70/Hsp90 organizing protein) occurs under heat shock, and its proposed nuclear localization signal is involved in Hsp90 binding. *Biochim. Biophys. Acta* **2008**, 1783 (6), 1003–14.
  - (39) Cappellini, A.; Chiarini, F.; Ognibene, A.; McCubrey, J. A.; Martelli, A. M. The cyclin-dependent kinase inhibitor roscovitine and the nucleoside analog sangivamycin induce apoptosis in caspase-3 deficient breast cancer cells independent of caspase mediated P-glycoprotein cleavage: implications for therapy of drug resistant breast cancers. *Cell Cycle* **2009**, 8 (9), 1421–5.

PR100468W